DNA Binding Mode and Sequence Specificity of Piperazinylcarbonyloxyethyl Derivatives of Anthracene and Pyrene

Hans-Christian Becker* and Bengt Nordén

Contribution from the Department of Physical Chemistry, Chalmers University of Technology, S-412 96 Gothenburg, Sweden

Received June 2, 1999

Abstract: Four novel piperazinylcarbonyloxyethyl derivatives of anthracene and pyrene have been prepared and investigated with respect to sequence specificity and synergism between hydrophobic and electrostatic effects upon binding to DNA. Linear and circular dichroism spectroscopy was used to assess the orientation of the aromatic chromophores relative to the nucleobases. Anthracene and pyrene derivatives **2a** and **3** are both concluded to bind to homo-polynucleotide poly(dA-dT)$_2$ by intercalation of their aromatic moieties between base pairs, with a binding constant K_{AT} of 4×10^5 M^{-1} and 2×10^6 M^{-1}, respectively. Significantly reduced affinities ($K_{GC} = 3 \times 10^4$ M^{-1} and 10^5 M^{-1}, respectively) are observed with poly(dG-dC)$_2$, due to less favorable interactions of the piperazinium tail in the minor groove. Base pair specificity is reflected in the binding thermodynamics, with the binding to AT being more enthalpically driven than the binding to GC. Phenyl substitution at the quaternary piperazinium site of the anthracene derivative **2b**, does not affect the ratio K_{AT}/K_{GC}, but reduces the affinity for both AT and GC slightly. Moreover, the phenyl group in the 10-position of **4** prevents intercalation, and apparently, this compound binds externally to both AT and GC duplex polynucleotides. The results are discussed in terms of general features of the interactions of the intercalating and minor-groove binding molecular moieties, and their interplay with each other, with potentials for tuning specificity.

Introduction

Cationically substituted polycyclic aromatic hydrocarbons, such as those derived from anthracene and pyrene, generally bind to DNA relatively nonspecifically by intercalation between base pairs.[1,2] A certain degree of specificity, attributed to electrostatic interactions with the DNA bases, has been observed for heterocyclic intercalators.[1,3−5] The base pair selectivity can be further enhanced by substituting the intercalators,[1,6] although minor variations in structure can have a pronounced influence on the binding specificity.[7−12] For certain natural products, the selectivity has been shown to be an inherent feature of the intercalating ring system.[13]

Intercalators that have some degree of sequence specificity are generally found to bind more strongly to GC than to AT. However, some alkylammonium substituted compounds, such as **1** (**1a**: Ar = 9-anthryl; **1b**: Ar = 9-phenanthryl; **1c**: Ar = naphthothiophene) have been found to be AT selective.[1]

Ar−CH(OH)CH$_2$N(CH$_2$CH$_2$OH)$_2$·HCl (**1a−c**)

It was assumed that the origin of such selectivity could be found in the interaction between the cationic tail and the minor groove of DNA.[1] An increase in DNA viscosity upon intercalation, due to elongation of the DNA helix, was found to be significantly smaller for the anthracene derivative **1a** than for **1b** and **1c**. The behavior of **1a** was attributed to bending of the DNA at the intercalation site.[1]

To improve our understanding of specificity and binding interactions of combined intercalators/groove-binders, we prepared a series of water-soluble piperazinylcarbonyloxyethyl derivatives **2−4** of anthracene and pyrene and investigated their interactions with DNA using linear and circular dichroism spectroscopy.

We expected the aryl moiety to be intercalated and, in conjunction with electrostatic attractions, the piperazinium tail to be pulled deep into the minor groove of the DNA double helix. The idea is to achieve sequence specificity by tuning steric and hydrophobic interactions of the intercalated aromatic moiety and the tailing, minor groove bound group. The orientation of the aromatic chromophores relative to the DNA was assessed by polarized spectroscopy.[14,15]

(1) Wilson, W. D.; Wang, Y.-H.; Kusuma, S.; Chandrasekaran, S.; Yang, N. C.; Boykin, D. W. *J. Am. Chem. Soc.* **1985**, *107*, 4989−4995.
(2) Kumar, C. V.; Asuncion, E. H. *J. Am. Chem. Soc.* **1993**, *115*, 8547−8553.
(3) Müller, W.; Crothers, D. M. *Eur. J. Biochem.* **1975**, *54*, 267−277.
(4) Strekowski, L.; Mokrosz, J. L.; Wilson, W. D.; Mokrosz, M. J.; Strekowski, A. *Biochemistry* **1992**, *31*, 10802−10808.
(5) Miller, K. J.; Newlin, D. D. *Biopolymers* **1982**, *21*, 633−652.
(6) Müller, W.; Crothers, D. M. *Eur. J. Biochem.* **1975**, *54*, 279−291.
(7) Atwell, G. J.; Baguley, B. C.; Denny, W. A. *J. Med. Chem.* **1988**, *31*, 774−779.
(8) Atwell, G. J.; Bos, C. D.; Baguley, B. C.; Denny, W. A. *J. Med. Chem.* **1988**, *31*, 1048−1052.
(9) Palmer, B. D.; Rewcastle, G. W.; Atwell, G. J.; Baguley, B. C.; Denny, W. A. *J. Med. Chem.* **1988**, *31*, 707−712.
(10) Rewcastle, G. W.; Denny, W. A.; Baguley, B. C. *J. Med. Chem.* **1987**, *30*, 843−851.
(11) Atwell, G. J.; Rewcastle, G. W.; Baguley, B. C.; Denny, W. A. *J. Med. Chem.* **1987**, *30*, 664−669.
(12) Atwell, G. J.; Cain, B. F.; Baguley, B. C.; Finlay, G. J.; Denny, W. A. *J. Med. Chem.* **1984**, *27*, 1481−1485.
(13) Bailly, C.; Waring, M. J. *Biochemistry* **1993**, *32*, 5985−5993.
(14) Nordén, B. *Appl. Spectrosc. Rev.* **1978**, *14*, 157−248.
(15) Nordén, B.; Kubista, M.; Kurucsev, T. *Quart. Rev. Biophys.* **1992**, *25*, 51−170.

10.1021/ja991844p CCC: $18.00
Published on Web 12/10/1999

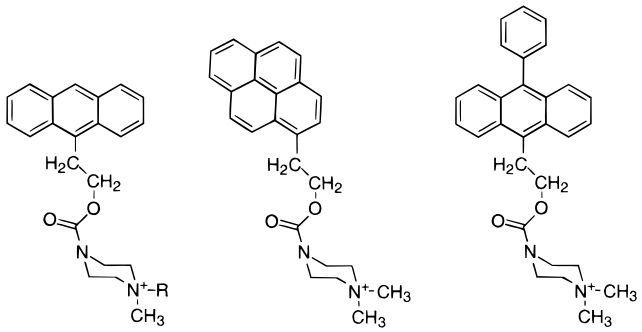

Experimental Section

Materials. Anthracene and pyrene derivatives **2**−**4** were prepared as outlined in Scheme 1. 2-(9-Anthryl)ethyl chloroformate[16,17] (**5**; Ar = 9-anthryl) and 2-(1-pyrenyl)ethyl chloroformate[18] (**5**; Ar = 1-pyrenyl) have been reported previously. 2-(10-Phenyl-9-anthryl)ethyl chloroformate **5c** was prepared in analogous fashion from phosgene and 10-phenyl-9-anthrylethanol. **5c** forms colorless crystals, mp 128 °C. ^{1}H NMR ($CDCl_3$) δ 8.33 (d, J = 9.0 Hz, 2H); δ 7.69 (d, J = 9.0 Hz, 2H); δ 7.56 (m, 5H); δ 7.37 (m, 4H); δ 4.73 (t, J = 8.9 Hz, 2H); δ 4.17 (t, J = 8.9 Hz, 2H).

Reaction of 1-methylpiperazine with 2-(9-anthryl)ethyl chloroformate as previously[19] reported for the derivatization of 1-phenylpiperazine, and 2-(1-pyrenyl)ethyl chloroformate gave the corresponding arylethyloxycarbonyl-4-methylpiperazines **6**. The piperazinylcarbonyloxyethyl derivatives **6** are characterized as follows. **6**, Ar = 9-anthryl, R = methyl: greenish-yellow crystals, mp 110 °C. ^{1}H NMR ($CDCl_3$) δ 8.39 (d, J = 8.1 Hz, 2H); δ 8.35 (s, 1H); δ 8.02 (d, J = 8.1 Hz, 2H); δ 7.54 (m, 2H); δ 7.47 (m, 2H); δ 4.50 (t, J = 8 Hz, 2J); δ 4.0 (t, J = 8 Hz, 2H); δ 3.51 (s, broad, 2H); δ 3.30 (s, broad, 2H); δ 2.37 (s, broad, 2H); δ 2.28 (s, 3H); δ 2.21 (s, broad, 2H). **6**, Ar = 1-pyrenyl, R = methyl: colorless crystals, mp 124 °C. ^{1}H NMR ($CDCl_3$) δ 8.35 (d, J = 9.3 Hz, 2H); δ 8.18 (d, J = 7.5 Hz, 2H); δ 8.14 (d, J = 9.3 Hz, 1H); δ 8.13 (d, J = 7.5 Hz, 1H); δ 8.04 (s, 2H); δ 8.00 (t, J = 7.5 Hz, 1H); δ 7.90 (d, J = 7.5 Hz, 1H); δ 4.53 (t, J = 7.2 Hz, 2H); δ 3.69 (t, J = 7.2 Hz, 2H); δ 3.50 (s, broad, 2H); δ 3.39 (s, broad, 2H); δ 2.35 (s, broad, 2H); 2.25 (s, 3H); δ 2.15 (s, broad, 2H). **6**, Ar = 10-phenyl-9-anthryl, R = methyl: pale yellow crystals, mp 151 °C. ^{1}H NMR ($CDCl_3$) δ 8.44 (d, J = 8.9 Hz, 2H); δ 7.66 (d, J = 8.9 Hz, 2H); δ 7.55 (m, 5H); δ 7.41 (m, 2H); δ 7.34 (m, 2H); δ 4.56 (t, J = 7.9 Hz, 2H); δ 4.08 (t, J = 7.9 Hz, 2H); δ 3.55 (s, broad, 2H); δ 3.38 (s, broad, 2H); δ 2.39 (s, broad, 2H); δ 2.29 (s, 3H); δ 2.26 (s, broad, 2H).

The preparation of **2a**, **3**, and **4** was accomplished by stirring a solution of **6** (0.3 mmol) and methyl iodide (1 mL) in acetonitrile (5 mL) overnight. Vacuum evaporation of solvent and excess methyl iodide afforded an oily residue, which was dissolved in a small amount of dichloromethane. Compounds **2a** (yellow crystals, mp 249−251 °C), **3** (colorless crystals, mp 219−221 °C), and **4**, (yellow crystals, mp 263−270 °C) crystallized upon addition of ether. The reaction of methyl iodide with the phenylpiperazine derivative **6** (Ar = 10-phenyl-9-anthryl, R = methyl) to give **2b** (yellow crystals, mp 186−190 °C) was carried out at 80 °C in an autoclave. Positive ion electrospray (90% CH_3OH, 9% H_2O, 1% acetic acid mobile phase) mass spectrometric analysis analysis yielded the following molecular ion masses. **2a**: 363.208 (calcd 363.207); **2b**: 425.220 (calcd 425.223); **3**: 387.208 (calcd 387.207); **4**: 439.240 (calcd 439.238); **7**: 250.160 (calcd 250.160).

Scheme 1

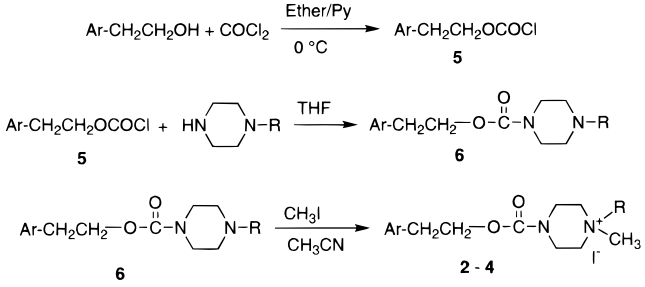

(9-Anthrylmethyl)trimethylammonium iodide (**7**) was prepared by stirring a solution of 9-(methylaminomethyl)anthracene (100 mg; 0.45 mmol) and methyl iodide (2 mL) in acetonitrile (75 mL) in the presence of sodium carbonate (100 mg) overnight at room temperature. The inorganic material was removed by filtration. Vacuum evaporation of solvent afforded a yellow solid, which was recrystallized from hot methanol. Yellow crystals, mp about 190 °C dec.

Calf thymus DNA was purchased from Sigma and used without further purification. Poly(dAdT)$_2$ (AT) and poly(dGdC)$_2$ (GC) were purchased from Pharmacia.

All measurements were performed at 20 °C in pH 7.2 buffer solution containing 10 mM NaCl, 5 mM Tris, and 1 mM sodium cacodylate. DNA and polynucleotide concentrations were determined spectrophotometrically, using $\epsilon_{260\ nm}$ = 6600 M^{-1} cm^{-1} for AT and calf thymus DNA, and $\epsilon_{254\ nm}$ = 8400 M^{-1} cm^{-1} for GC. Absorption spectra were recorded on a Cary 4B spectrophotometer, LD spectra on Jasco J-500A and J-710 spectropolarimeters equipped with an Oxley prism for LD measurement, and CD spectra on a Jasco J-710 spectropolarimeter. Absorbance titrations of the ligands were carried out by adding aliquots of a concentrated DNA solution. Titration end points were, whenever possible, determined by using a large excess of polynucleotide. When the binding constant was too low to allow complete complexation, the spectrum of the complexed ligand was constructed by linear combination of the spectra of the free ligand, and that of a mixture of free and bound ligand. The correct combination coefficients were determined by visual inspection of the resulting absorption spectra and the corresponding LD^r spectra. To determine the binding isotherms, the spectra from the titrations were least-squares-fitted to the spectra of free and bound ligand. Except for the titrations of **4**, singular value decomposition analysis of the absorption spectra in the 300−450 nm region gave no more than two significant components, corresponding to free and bound ligand. Binding constants and binding site widths were assessed from absorbance titrations using the method of McGhee and von Hippel.[20,21] We tried to include cooperativity when fits were only fair, but since the fits did not improve, we chose the noncooperative model for the analyses.

As the low affinitites of **2** and **3** for GC made calorimetric determinations of the heat of binding difficult, binding enthalpies and entropies were determined from van't Hoff plots. Concentrations of polynucleotide and ligand were chosen so as to give approximately 50% bound ligand at 20 °C. Binding constants were determined as described above. No significant deviations from linearity were observed in the van't Hoff plots between 5 and 50 °C. The van't Hoff enthalpies are in agreement with calorimetrically determined heats of binding of **2** and **3** to calf thymus DNA, suggesting that the change in heat capacity on binding is small. Above 50 °C, melting of poly[dA-dT] was observed. We have not specifically determined the stabilization of AT and GC by **2**−**3**, but the data from the van't Hoff plots give an indication of the influence of **2** and **3** on the duplex stability. The partitioning of the free energy of binding into a polyelectrolyte part ($\Delta G°_{pe}$) and a nonpolyelectrolyte part ($\Delta G°_{npe}$) was done using eq 1.[22−25]

(16) Sörensen, H. F, Ph.D. Thesis, University of Gothenburg: Gothenburg, 1988.
(17) Faulkner, A. J.; Veening, H.; Becker, H.-D. *Anal. Chem.* **1991**, *63*, 292−296.
(18) Cichy, M. A.; Stegmeier, D. L.; Veening, H.; Becker, H.-D. *J. Chromatogr.* **1993**, *613*, 15−21.
(19) Becker, H.-D.; Burgdorff, C.; Löhmannsröben, H.-G. *J. Photochem. Photobiol., A* **1995**, *86*, 133−139.
(20) McGhee, J. D.; von Hippel, P. H. *J. Mol. Biol.* **1974**, *86*, 469−489.
(21) McGhee, J. D.; von Hippel, P. H. *J. Mol. Biol.* **1976**, *103*, 679.
(22) Chaires, J. B.; Priebe, W.; Graves, D. E.; Burke, T. G. *J. Am. Chem. Soc.* **1993**, *115*, 5360−5364.
(23) Chaires, J. B.; Satyanarayana, S.; Suh, D.; Fokt, I.; Przewloka, T.; Priebe, W. *Biochemistry* **1996**, *35*, 2047−2053.
(24) Hopkins, H. P.; Wilson, W. D. *Biopolymers* **1987**, *26*, 1347−1355.

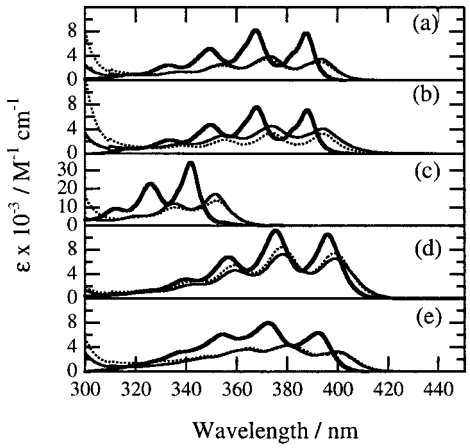

Figure 1. Absorption spectra of compounds **2**−**4** and **7**. The thick solid lines are the spectra of the free compounds. The spectra of the complexes are given by the thin solid (AT) and dotted (GC) lines. (a) **2a**, (b) **2b**, (c) **3**, (d) **4**, (e) **7**. The spectra of the bound ligands were obtained at a DNA:ligand ratio of >40, and the spectrum of the free ligand subtracted, as described in the text.

$$\Delta G^{\circ}_{pe} = -RT \ln[\mathrm{Na}^+] \frac{\partial \ln K}{\partial \ln[\mathrm{Na}^+]} \qquad (1)$$

Results

Absorption Spectra. In the presence of DNA and double-helical polynucleotides, compounds **2**−**4** show absorption spectra with extensive hypochromism and red-shifts (Figure 1), indicating strong interaction between the aromatic chromophores and the DNA bases. Isosbestic points are exhibited in absorbance titrations of **2a**, **2b**, and **3** with AT and GC, suggesting that only two species, namely, free (uncomplexed) and bound ligand, are spectroscopically distinguishable. This justifies the application of a two-state model for describing the binding process of compounds **2** and **3**. Significantly, titration spectra of the phenylanthracene derivative **4** with AT and GC are characterized by the lack of isosbestic points, which here indicates multiple binding modes. It also appears that the bathochromic shift of **4** upon binding to DNA is smaller (∼200 cm^{-1}) than for compounds **2** and **3** (400−800 cm^{-1}), indicating that the binding geometry of **4** differs significantly from that of **2** and **3**. The LD and CD results discussed below support this conclusion.

Linear and Circular Dichroism. LD spectra of compounds **2**−**4** were first recorded using calf thymus DNA, which by its greater contour length and better flow-orientation properties gives much larger LD amplitudes than the synthetic polynucleotides. The reduced dichroism was then formed as LD^r = LD/A_{iso}. From the spectra (Figure 2), it appears that only compound **2a** shows ligand orientation properties fully consistent with intercalation into DNA. As to the **2b**−DNA complex, the noticeably wavelength-dependent LD^r is at variance with a homogeneous intercalative binding. The less negative LD^r around 250 nm, where there is a strong, long-axis polarized anthracene transition, may suggest that the anthracene long-axis in **2b** is not perfectly perpendicular to the DNA helix axis. For the pyrene derivative **3**, we observe an enhanced wavelength dependence of the LD^r. Such strong variation in LD^r with wavelength indicates that there are at least two binding modes, characterized by different absorption spectra. Contrasting the behavior of **2** and **3**, the phenylanthracene **4** shows very little LD, indicating neither intercalation nor groove binding.

As a reference, we have also investigated the interaction of DNA with a structurally simple anthrylalkylammonium salt,

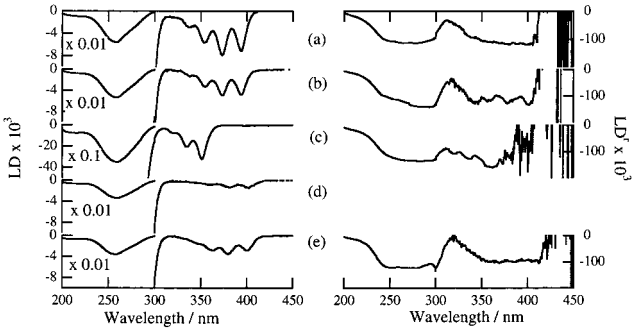

Figure 2. Linear dichroism (left panel) and reduced linear dichroism (right panel) of compounds **2**−**4** and **7** bound to calf thymus DNA. (a) **2a**, (b) **2b**, (c) **3**, (d) **4**, (e) **7**. Binding ratios were ca. 50 (DNA:ligand).

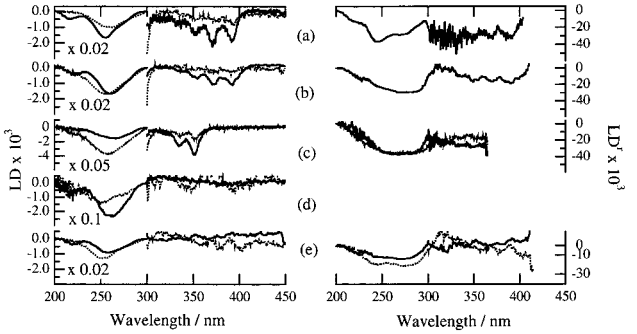

Figure 3. Linear dichroism (left panel) and reduced linear dichroism (right panel) of compounds **2**−**4** and **7** bound to AT (solid lines), and GC (dotted lines). (a) **2a**, (b) **2b**, (c) **3**, (d) **4**, (e) **7**. Binding ratios were ∼40 (DNA:ligand).

namely, (9-anthrylmethyl)trimethylammonium iodide (**7**). For this compound, the LD^r in the 310−400 nm region does indicate intercalation, although the LD^r is not quite as negative as that in the DNA band.

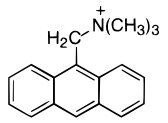

7

Further insight into the binding modes of **2**−**4** was gained by LD, CD, and absorption spectra of the ligand−polynucleotide complexes. Figure 3 shows the LD and LD^r spectra of the complexes with AT and GC. Despite the small signals (poor orientation due to short polynucleotides), the spectra allow the following conclusions. Anthracene derivatives **2a** and **2b** intercalate into AT, while their binding mode to GC is less obvious (see Discussion). The pyrene derivative **3** intercalates into AT, and probably also into GC. Different from **2** and **3**, the phenylanthracene **4** shows virtually no LD when bound to either AT or GC. Model anthracene compound **7** intercalates at least partially into GC, but shows very little LD when bound to AT. This means that **2** and **3** intercalate into AT, while **7**, lacking the piperazinium moiety, intercalates into GC. All complexes show very little induced CD (Table 1), as is expected for intercalation or random external binding.[26]

Binding Constants. Binding affinities as well as site widths for the complexes with AT and GC are summarized in Table 2. We are aware that the limited saturation range makes the uncertainty in the binding values larger than desirable, but the

(25) Wilson, W. D.; Lopp, I. G. *Biopolymers* **1979**, *18*, 3025−3041.

(26) Lyng, R.; Rodger, A.; Nordén, B. *Biopolymers* **1991**, *31*, 1709−1820.

Table 1. Induced CD Features of $\pi \rightarrow \pi^*$ Transitions in AT and GC Complexes of Compounds **2**−**4**

compound	[(poly(dA-dT)]$_2$	[(poly(dG-dC)]$_2$
2a	positive (310−400 nm)	positive (310−400 nm)
2b	positive (310−400 nm)	positive (310−400 nm)
3	negative (310−370 nm)	positive (310−370 nm)
4	none (300−400 nm)	none (300−400 nm)

Table 2. Binding Constants and Binding Site Widths as Determined from McGhee−von Hippel Analysis of Absorbance Titrations

	[(poly(dA-dT)]$_2$		[(poly(dG-dC)]$_2$	
compound	K/M^{-1}	n/bp	K/M^{-1}	n/bp
2a	$4 \times 10^5 \pm 10^5$	2.3 ± 0.3	$3 \times 10^4 \pm 10^4$	2.1 ± 0.1
2b	$2 \times 10^5 \pm 10^5$	1.9 ± 0.3	*ca.* 10^4	*ca.* 2
3	$2 \times 10^6 \pm 5 \times 105$	2.6 ± 0.3	*ca.* 10^5	2−3
4	*a*	*a*	*a*	*a*
7	$2 \times 10^5 \pm 10^5$	2.0 ± 0.3	$3 \times 10^5 \pm 10^5$	2.3 ± 0.3

[a] Heterogeneous binding.

Table 3. Thermodynamic Parameters[a] for the Binding of **2**−**3** and **7** to AT and GC[b]

	[(poly(dA-dT)]$_2$				[(poly(dG-dC)]$_2$			
compound	$\Delta G°_{pe}$	$\Delta G°_{npe}$	$\Delta H°$	$-T\Delta S°$	$\Delta G°_{pe}$	$\Delta G°_{npe}$	$\Delta H°$	$-T\Delta S°$
2a	−2.9	−4.1	−5.2	−1.8	−2.8	−2.7	−2.7	−2.8
2b	−2.3	−4.7	−6.1	−0.9	−2.4	−2.4	−3.8	−1.0
3	−2.6	−5.5	−8.2	+0.08	−2.7	−3.9	−5.1	−1.5
7	−2.3	−4.7	−2.9	−4.1	−2.5	−4.4	−2.5	−4.4

[a] In kcal/mol at 20 °C and 10 mM NaCl. [b] $\Delta G°_{pe}$ denotes the polyelectrolyte contribution to the free energy of binding, and $\Delta G°_{npe}$ is the difference between $\Delta G°_{obs}$ and $\Delta G°_{pe}$.

small binding constants together with the relatively low extinction coefficients of **2** and **7** preclude a higher saturation coverage. Despite this, the data in Table 2 should give a good description of the relative affinities for AT and GC of **2a**, **2b**, **3,** and **7**. The binding site widths obtained for compounds **2** and **3** are compatible with the nearest-neighbor exclusion model, as was also found for similar systems.[1] Although some of the fits are only fair, we conclude that **2** and **3** are characterized by significantly different affinities for AT and GC. The largest preference for AT compared to GC, namely 20-fold (corresponding to a difference of 2 kcal/mol in binding free energy), is found for **2a**. By contrast, the anthrylalkylammonium model compound **7** shows virtually no base pair preference.

Thermodynamics. Thermodynamic parameters for the binding of **2** and **3** to AT and GC are collected in Table 3 and Figure 4. The corresponding van't Hoff plots are shown in Figure 5. For compounds **2**, **3**, and **7**, the binding to both AT and GC is enthalpically favored. The AT specificity observed for **2** and **3** is reflected in the magnitude of the binding enthalpies. The heats of binding of **2a**, **2b**, and **3** to AT are more than 60% more negative than for the corresponding binding to GC. The $T\Delta S°$ contribution is not as systematically affected as $\Delta H°$, but the binding to AT is in general entropically disfavored compared to the binding to GC. The differences in binding enthalpy and entropy for **7**:AT and **7**:GC are small. This observation suggests that the AT specificity of **2** and **3** manifests itself in the heat of binding.

As compounds **2**, **3**, and **7** do not bind strongly to single-stranded DNA, we can from the point in the van't Hoff plots where the binding constant (amount of bound ligand) drops sharply estimate the difference in melting temperature of the AT complexes of **2**, **3**, and **7**. At a total concentration of 80 μM bases AT a sharp increase in free ligand concentration occurs at ∼50 °C for **2a**:AT and **2b**:AT, and at ∼55 °C for **7**:AT. For **3**:AT, at a concentration of 40 μM AT, the release of ligand occurs at about 60 °C. Thus, the degrees of AT stabilization appear to be **2a** ≈ **2b** < **7** ≪ **3**.

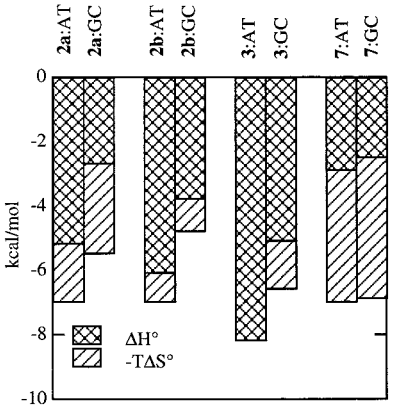

Figure 4. Enthalpic and entropic contributions to the binding of **2**−**3** and **7** to AT and GC. Concentrations were chosen as to give ∼50% bound ligand at 20 °C, with total concentrations of ∼6 μM (**2** and **7**), and 3 μM (**3**).

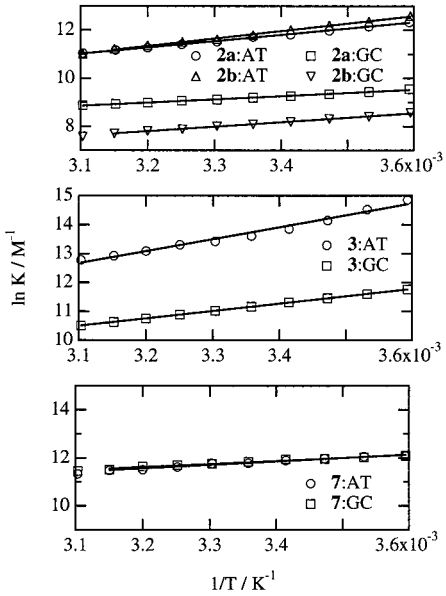

Figure 5. van't Hoff plots for the binding of **2**−**3** and **7** to AT and GC.

For compounds **2**, **3**, and **7**, the slopes $(\partial \ln K)/(\partial \ln[Na^+])$ were around −1 (data not shown) for both AT and GC complexes, indicating similar polyelectrolyte binding free energies of about −2.5 kcal/mol.

Discussion

The results indicate that compounds **2** and **3** intercalate with a high specificity for AT. The phenyl-substituted anthracene **4** shows multiple binding modes to both AT and GC, but absorbance titrations show that the affinity is of the same order of magnitude as that of **2**.

Since neither (9-anthrylmethyl)ammonium chloride,[2] nor the analogous model compound **7** shows any significant base pair preference, we attribute the selectivity of **2** and **3** to interaction between the piperazinium site and the DNA. We base this conclusion on the following observation. The similarity of the induced CD spectra of the complexes **2**−DNA and **7**−DNA indicate similar binding geometries. Thus, the relatively large

separation of the cationic site and the intercalating moiety in **2** compared to **7** does not change the intercalation properties. Furthermore, the origin of the sequence specificity is not due to the charge itself, but to the fact that the charge causes the piperazinium side-chain to reside inside the minor groove.

One may argue that AT and GC are not very good models of the binding sites found in mixed-sequence DNA and that the difference in affinitites merely reflect the different helical stabilities of AT and GC. The AT specificity of the neutral intercalator 7,8,9,10-tetrahydroxy-7,8,9,10-tetrahydrobenzo[*a*]-pyrene has been attributed to this.[27,28] While intrinsic differences in the intercalation pockets of AT and GC may induce sequence specificity in neutral intercalators, the consequences of pulling the piperazinium tail in **2**, **3**, and **7** into the minor groove via the charge will probably have a larger effect on the binding than differences in, for example, unwinding stability and polarizability, between AT and GC. Furthermore, the observations that only **2** and **3** show AT-specific binding, while **7** does not, along with the significant difficulty of saturating calf thymus DNA, also speak in favor of true AT preference. Had factors such as different unwinding resistance been important, those would have affected the binding of **7** too, as well as that of **2**.

The driving force for the binding of compounds **2**−**4** may be assumed to consist of two parts: (1) hydrophobic/dispersive interactions associated with intercalative stacking of the aromatic ring system with the base pairs and (2) the interaction of the piperazinium tail with the minor groove of DNA. While the former part is of predominantly attractive nature, the latter involves both attractive electrostatic interactions, including hydrogen bonding, as well as steric repulsion. The pyrene derivative **3** binds 10 times more strongly to DNA than anthracene derivatives **2**. This is in line with previous investigations, in which the importance of good overlap of intercalator and base pair has been recognized.[29] As for the only slightly decreased affinity of **2b** compared to that of **2a**, this indicates a rather unsignificant interference of the phenyl substituent in **2b** and the DNA as to steric demands and hydrophobic interaction with the hydrated minor groove.[30,31] Since K_{AT}/K_{GC} is virtually the same for **2a** and **2b**, we are therefore inclined to believe that the phenyl interacts primarily with the exterior of the DNA (such as the backbone), rather than with the more sequence-dependent interior of the groove.

The LD and LD^r spectra of compounds **2** and **3** bound to calf thymus DNA support for all of them an intercalative binding mode. This is interesting in view of the large difference in binding affinities for AT and GC, and the poor LD observed with the latter polynucleotides. As the affinity for AT is about 20 times higher, and the LD spectra were recorded with a relatively large excess of DNA of about 20 base pairs per ligand, the LD spectra will probably to a high degree reflect the binding of the compounds to AT-rich regions.

There remains the question concerning the binding mode of **2** to GC. The LD and LD^r obtained for the calf thymus DNA complexes of **2** can, as noted above, not necessarily be applied for determining the binding mode. We conclude from the strong interaction between the anthracene π-system and the DNA bases, evidenced from the absorption features, that **2** and **3** intercalate into GC. The weak LD signal of the GC complexes of **2** is not readily explained. It is conceivable that the affinity for GC is too low to allow accurate measurement of LD at reasonable poly(dG-dC)$_2$ concentrations. However, the LD spectra of **2**-AT and **2**-GC were recorded at 17 and 10 μM bound ligand, respectively, so that it can most likely be ruled out that the difference in LD signal is due to different concentrations of bound **2**. A remaining explanation is that the anthracene derivatives **2** have a binding mode where the aryl moiety is only partially inserted into the intercalation pocket. This interpretation is supported by fluorescence anisotropy (FA, λ_{em} = maximum of the emission, λ_{ex} = 300−420 nm, lifetimes are ~5 ns) measurements. For the AT complexes, we find $r < 0.05$, indicating that the chromophore has a high degree of motional freedom during its excited state lifetime. GC efficiently quenches the anthracene emission, so that the FA measurements in these cases were inconclusive. We believe that the anthracene, due to steric clashing between the lateral rings and the DNA backbone cannot intercalate with its short-axis parallel to the base pair long axis. It seems likely that the intercalation involves insertion of a lateral ring into the DNA. Similar arguments have been presented earlier.[1] The observed increasingly more negative LD^r of **2a**−DNA toward the red end of the absorption spectrum could indicate that the anthracene short-axis is more perpendicular to the DNA helix axis than the long-axis.[32] Such a binding mode would not be very rigid, as it involves only limited overlap of the base pair and the anthracene. Thus, any interference of the piperazinium with the minor groove of the DNA could have a pronounced effect on the spatial insertion of the anthracene. Such a decrease of overlap will consequently reduce the anthracene−base pair interactions. Still, even the limited overlap of the anthracene with the DNA bases can have the observed spectroscopic repercussions.

The heterogeneous binding of **4** concluded above can be understood in terms of the molecular geometry of the 10-phenylanthracene moiety. It is known from X-ray crystallographic systematic studies of steric and conjugation effects that the phenyl ring and the anthracene are practically perpendicular to each other.[33] Consequently, intercalation of **4** is effectively prevented by spatial interference. This conclusion, together with an increased hydrophobic character upon introducing the phenyl moiety, can explain the disordered, possibly external binding modes of **4** that are evidenced from the linear dichroism results.

A more detailed description of the intercalation geometry can be obtained from the sign of the induced CD spectra (Table 1). In anthracene derivatives **2a** and **2b**, the positive induced CD of both their AT and GC complexes supports a binding mode with the molecular short-axis parallel to the long-axis of the base-pair. The pyrene derivative **3** is interesting insofar as **3**-AT and **3**-GC differ in the sign of the induced CD in the long-axis polarized L_a band at 350 nm. The **3**-AT complex shows a negative induced CD signal, suggesting that the molecular long-axis is oriented along the base-pair long-axis.[26,34,35] By contrast, **3**-GC exhibits a positive induced CD, which indicates a different orientation in the intercalation pocket. Although it is difficult to assess absolute binding geometries, the intercalation mode

(27) Geacintov, N. E.; Shabaz, M.; Ibanez, V.; Moussaoui, K.; Harvey, R. G. *Biochemistry* **1988**, *27*, 8380−8387.
(28) Shimer, G. H., Jr.; Wolfe, A. R.; Meehan, T. *Biochemistry* **1988**, *27*, 7960−7966.
(29) Kool, E. T.; Matray, T. J. *J. Am. Chem. Soc.* **1998**, *120*, 6191−6192.
(30) Jóhannesson, H.; Halle, B. *J. Am. Chem. Soc.* **1998**, *120*, 6859−6870.
(31) Shui, X.; McFail-Isom, L.; Hu, G. G.; Williams, L. D. *Biochemistry* **1998**, *37*, 8341−8355.
(32) Michl, J.; Thulstrup, E. W. *Spectroscopy With Polarized Light. Solute Alignment by Photoselection, in Liquid Crystals, Polymers, and Membranes*, 2nd ed.; VCH Publishers: Weinheim, 1995.
(33) Becker, H.-D.; Langer, V.; Sieler, J.; Becker, H.-C. *J. Org. Chem.* **1992**, *57*, 1883−1887.
(34) Schipper, P. E.; Nordén, B.; Tjerneld, F. *Chem. Phys. Lett.* **1980**, *70*, 17−21.
(35) Nordén, B.; Tjerneld, F. *Biopolymers* **1982**, *21*, 1713−1734.

of the AT complex probably involves a large overlap of pyrene and base pair. By contrast, in the **3**-GC complex, we may anticipate from the sign of the induced CD that the pyrene short-axis is parallel to the base pair long-axis. Consequently, the decrease in intercalator overlap lowers the affinity.

The binding thermodynamics supports the conclusion that **2** and **3** should intercalate with different depths in AT and GC. An indication of the greater base pair overlap of **3** compared to **2** and **7** can be found in the more than 10 °C higher melting temperature of **3**:AT compared to those of **2**:AT and **7**:AT. Furthermore, the significant difference in the ratio $\Delta H°/-T\Delta S°$ between the AT and GC complexes can be interpreted in terms of a balance between deep intercalation with a restricted motional space, and less tight binding with a larger conformational manifold.

Among the contributions to the binding enthalpy and entropy, we will consider the following. (1) The disruption of the water structure around the aromatic moiety and solvation shell of the cationic site upon intercalation will constitute a positive contribution to the binding entropy. (2) The above process will also contribute to the binding enthalpy. Although the release of "hydrophobic water" involves the breaking of hydrogen bonds, those are weaker than those that are re-formed in the bulk.[36] By contrast, the disruption of the ion solvation shell will form an unfavorable contribution. The net effect, however, is most likely favorable, judging from the significantly more favorable binding enthalpy of **3** compared to that of **2**. On the basis of this observation, we also conclude that the significantly different binding enthalpies of the AT and GC complexes of **2** and **3** are due to the different intercalation depths. As for the entropic effects, the release of bound water and ions will give a positive contribution to the binding entropy. Furthermore, the change in motional freedom of both DNA and ligand on binding will contribute to $\Delta S°$. These contributions are difficult to estimate, but since for both AT and GC complexes of **2**, **3**, and **7** the polyelectrolyte contribution to the free energy of binding (and thus the contribution to $\Delta S°$) is about the same, we conclude that the variations in the non-polyelectrolyte part of the binding entropy arise from the different degrees of motional freedom of the bound ligand.

We thus conclude that the thermodynamic arguments corroborate the binding of **2** and **3** to AT and GC as follows. In AT, the enthalpic gain by having a large overlap between intercalator and nucleobases is in part compensated by a more rigid binding mode. By contrast, the binding to GC involves a smaller degree of intercalation due to steric interference of the piperazinyl tail and the exocyclic amino groups of guanine in the minor groove. This reduces the magnitude of the binding enthalpy, but the less tight binding increases the binding entropy.

Conclusions

Piperazinylcarbonyloxyethyl substitution adds AT specificity to the binding interaction of both anthracene and pyrene. Synergistic effects may contribute to the observed selectivity: because of its spatial demand, the piperazine tail cannot penetrate as deep into the minor groove of GC, which contains the exocyclic guanine amino groups, as into that of AT, and the electrostatic attraction is thereby reduced. As a consequence, the piperazinium tail is forced out of the minor groove of GC, and this in turn impairs intercalation of the aromatic moiety. This decreases the overlap of the aromatic part with the base pair. Thermodynamic measurements reveal that the decrease in affinity is due to less favorable binding enthalpy. Phenyl substitution of the piperazinium site is found to have little effect on affinity and selectivity. However, phenyl substitution of the anthracene moiety prevents intercalation into DNA for steric reasons.

Acknowledgment. We are indebted to Dr. Gunnar Stenhagen for assistance with the mass spectroscopic analyses.

Supporting Information Available: McGhee−von Hippel binding isotherms and plots of ln K vs ln[Na^+] for AT and GC complexes of compounds **2**−**3** and **7** (PDF). This material is available free of charge via the Internet at http://pubs.acs.org.

JA991844P

(36) Becker, H.-C.; Nordén, B. *J. Am. Chem. Soc.* **1997**, *119*, 5798−5803.